

Water recovery and air humidification by condensing the moisture in the outlet gas of a proton exchange membrane fuel cell stack

Z.M. Wan^{a,c,*}, J.H. Wan^a, J. Liu^a, Z.K. Tu^{b,**}, M. Pan^b, Z.C. Liu^c, W. Liu^{c,*}

^a School of Physics and Electronic Engineering, Hunan Institute of Science and Technology, Yueyang, Hunan 414006, China

^b State Key Laboratory of Advanced Technology for Materials Synthesis and Processing, Wuhan University of Technology, Wuhan 430070, China

^c School of Energy and Power Engineering, Huazhong University of Science and Technology, Wuhan 430074, China

ARTICLE INFO

Article history:

Received 2 September 2011

Accepted 29 February 2012

Available online 13 March 2012

Keywords:

Proton exchange membrane fuel cells

Stack

Water recovery

Air self-sufficient in water

Condenser

ABSTRACT

Humidification is one of the most important factors for the operation of proton exchange membrane fuel cell (PEMFC). To maintain the membrane at hydrated state, plenty of water is needed for the state-of-the-art of PEMFC technology, especially in large power applications or long time operation. A condenser is introduced to separate liquid water from the air outlet for air self-sufficient in water of the stack in this study. The condensed temperature at the outlet of the condenser and water recovered amount for air self-sufficient in water are investigated theoretically and experimentally. It is shown that the condensed temperature for air self-sufficient in water is irrelevant with the working current of the stack. When the condenser outlet temperature was above the theoretical line, recovery water was not sufficient for the air humidification. On the contrary, it is sufficient while the temperature was below the theoretical line. It is also shown that when the moisture is sufficiently cooled, large amount water can be separated from the outlet gas, and it increased almost linearly with the time. With the introduction of the condenser, the recovered amount of water can easily satisfy the air self-sufficient in water by condensing the outlet gas to a proper temperature.

© 2012 Elsevier Ltd. All rights reserved.

1. Introduction

Proton exchange membrane fuel cell (PEMFC) has been considered to be one of the promising power sources for portable devices, transportation and stationary applications due to its high energy conversion efficiency, high power density, quick startup, and low environment pollution [1–3]. Many aspects of PEMFC, such as thermal management, temperature distribution, system optimization design et al., have been studied for years [4–9]. However, one critical requirement for operated PEMFC is to maintain high water content in the electrolyte to ensure reasonable ionic conductivity. Therefore, water molecules must be supplied continuously to prevent drying of the membrane as can lead to dramatic decrease in ionic conductivity. To date, a variety of methods have been developed to make the membrane well humidified, and they are mainly categorized into external humidification and internal humidification, respectively.

External humidification refers to the process that membranes are humidified by humidified reactants gases through humidifiers prior to flowing into the cell and the humidification process mainly takes place outside of the fuel cell stack [10–16]. Since this process is relatively easy to be handled, it has been the most commonly used technique. Lee et al. [10] investigated the effects of external humidification to the membrane by varying the humidification side such as anode humidification, cathode humidification, and both anode and cathode humidification (called as both-side humidification). The results showed that the best performance of the cell was achieved by both-side humidification. The higher temperature in the anode humidification resulted in the degraded performance of the cell. Jung et al. [11] developed a scaled gas humidification system using injectors for PEM fuel cell vehicles. The humidification system consisted of an injector, a duplex enthalpy mixer and a water management apparatus. Humidification performance was observed to be critically affected by the temperature of injected water and the gas flow rate in their study, and inlet gas temperature also affected the humidification performance and response time. Sridhar et al. [12] investigated the external membrane humidification in the anode. The results showed that the water of solvation of protons decreases with increase in the current density and the electrode area, and the coolant water itself can be used for

* Corresponding authors. School of Energy and Power Engineering, Huazhong University of Science and Technology, Wuhan 430074, China. Tel.: +86 27 87542618; fax: +86 27 87540724.

** Corresponding author. Tel.: +86 27 87651837; fax: +86 27 87879468.

E-mail addresses: zhongminwan@hotmail.com (Z.M. Wan), tzklq@whut.edu.cn (Z.K. Tu), w_liu@hust.edu.cn (W. Liu).

humidifying the hydrogen gas. Springer et al. [13] used an external humidification model to investigate the proton transport in the membrane, and the model predicts a net-water-per-proton flux ratio of $0.2\text{H}_2\text{O}/\text{H}^+$ under typical operating conditions. Nguyen and co-workers [14] have reported the effectiveness of the direct liquid water injection scheme and the interdigitated flow field design toward providing adequate gas humidification to maintain optimum membrane hydration and to alleviate mass-transport limitations of the reactants and electrode flooding. Hyun and Kim [15] investigated an external humidification method used in a fuel cell experiment. Humidity and temperature of the gas were measured using a dew point transmitter. E-tek electrode and Nafion 115 membrane were used to determine the relationship between relative humidity and cell performance. The results showed that the relative humidity of hydrogen gas was lower by about 10–15% than that of air or oxygen. Rajalakshmi and co-workers [16] investigated the water pick-up by various spargers in an external conventional humidifier under various operating conditions. Optimization of humidification was also discussed with respect to the pressure drop of the reactants while trying to achieve the theoretical relative humidity (RH), especially for the requirements of kilowatts stacks.

Internal humidification refers to the process that membranes are humidified by the generated water molecules from electrochemical reaction mainly using novel structure of self-humidified membrane and self-humidified structure of flow field [17–22]. Lee et al. [17] fabricated Pt/zirconium phosphate–Nafion composite membrane for self-humidified PEMFC applications. Water was produced by the crossover of hydrogen and oxygen onto Pt particles embedded in the membrane and the membrane can be therefore hydrated by the in situ generated water. The effects of the size, distribution and amount of Pt impregnated in the Nafion membrane were investigated in detail as well. Yang et al. [18] presented a self-humidifying membrane for the PEMFC by using copolymer resin and a sputtering technique and higher performance of self-humidifying cell was attributed due to the Pt particles in the membrane increases the proton conductivity of the membrane. Wang et al. [19] developed a self-humidifying reinforced composite membrane by sputtering Pt/SiO₂ catalyst particles uniformly into the Nafion resin, and compared with commercial Nafion® NRE-212, the cell performance was obviously improved. Santis et al. [20] using the product water from the exhaust air to humidify membrane indirectly and tests had shown that cells have almost the same performance as when operated with external humidification. Büchi and Srinivasan [21] proposed a model for the operation of PEMFC with internal humidification of the gases and the operating conditions for PEMFC using dry H₂/air were also investigated. The model predicted that dry air, entering at the cathode, could be fully internally humidified by the water produced by the electrochemical reaction at temperatures up to 70 °C. This model was experimentally verified for cell temperatures up to 60 °C by long-term operation of a PEMFC with dry gases for up to 1800 h. Ge et al. [22] investigated the performance of the internally humidified PEMFC using water absorbing sponge. Mounting the sponge wicks was advantageous for the humidification of dry inlet air and for the removal of liquid water in the cell. It was found that dry inlet hydrogen could be internally humidified by water diffusion from the cathode to anode when operating in a counter-flow mode.

As mentioned above, for internal humidification, the self-water balance in membrane can be achieved under restricted operating conditions with regard to gas flow rates and cell temperature or specific electrode/flow field design. However, practically it is quite difficult to control the relative humidity and this kind of humidification process is not appropriate for large systems, especially in automotive applications [11]. On the contrary, external

humidification method is widely used due to its simplicity [15]. However, large amount of water is needed to humidify the reactant gases, especially in large power applications or long time operation. Considering the safety and convenience, a condenser is applied to separate liquid water from the air outlet of the stack to demonstrate that it can be sufficient enough in water for the air humidification by condensing the moisture of the air outlet directly in this paper. The temperature of separation and recovered amount of water are investigated theoretically and experimentally as well.

2. Experiment

2.1. Experimental system

The PEM fuel cell stack used in this study is composed of 84 single cells using graphite plates as current collector with straight-channel flow field. Geometrical properties of PEM fuel cell stack are listed in Table 1. The used MEAs (Membrane Electrode Assembly) consisted of the composite polymer electrolyte membrane in combination with platinum loadings of 0.4 mg cm⁻² per electrode and the stack is cooled by the deionized water at a pre-set temperature. The performance of the stack was carried out on FCATS G500 produced by Greenlight Innovation Company in Canada. It could be programmed precisely to control various operational parameters, including electronic load, gas flow rate or stoichiometry, dew point temperature, inlet/outlet pressures, relative humidity (RH), and cell temperature. The air and hydrogen flow rate rangeability are 0–750 NLPM and 0–250 NLPM, respectively, and the measurement accuracy is ±0.1%. The current rangeability is 0–500 A with the accuracy ±0.1%, and the single cell voltage can be monitor at –1.500–+1.500 V. The schematic diagram of the test system for PEM fuel cell stack is shown in Fig. 1.

Although all the reactant gases are humidified by the G500, the rest hydrogen is exhausting directly into the atmosphere without condensing. Both pressure gauge and temperature sensor are placed at the air outlet of the condenser to monitor the outlet pressure and temperature. The pressure is measured by FCX-AII series differential pressure transmitter, and measurement accuracy is ±0.1%. The temperature is measured by a T-Type Temperature monitor (XMTD-3002) with the accuracy ±0.5 °C. The condenser is associated with two cooling fans while each fan can work independently. The rib material of the condenser is aluminum and the effective heat exchange area is 7.1 m², while the air flow rate of the fan is 500 L/Min at the rated voltage of 24 V and current of 8 A, respectively. The two-phase fluid flows into the bottom of the tank and the liquid water is collected by a measuring cylinder and for measurement convenience, and the measuring cylinder is filled with water of 400 mL for each case before the experiment. The rest gas exhausted from the top of the tank. The stack is cooled by the coolant water, and we will open the radiator manually when the coolant water temperature is about 338 K (65 °C). The schematic diagram of the self-humidification process and the detail test information of the condenser are shown in Fig. 2 and Table 2, respectively.

Table 1
Geometrical properties of PEM fuel cell stack.

Single cell area of this stack (m ²)	200×10^{-4}
Flow field depth (m)	1.0×10^{-3}
Flow field width (m)	1.0×10^{-3}
Flow field ridge width (m)	1.0×10^{-3}
Gas diffusion layer thickness (m)	2.5×10^{-4}
PEM thickness (m)	1.2×10^{-5}
Catalyst layer thickness (m)	1.2×10^{-5}

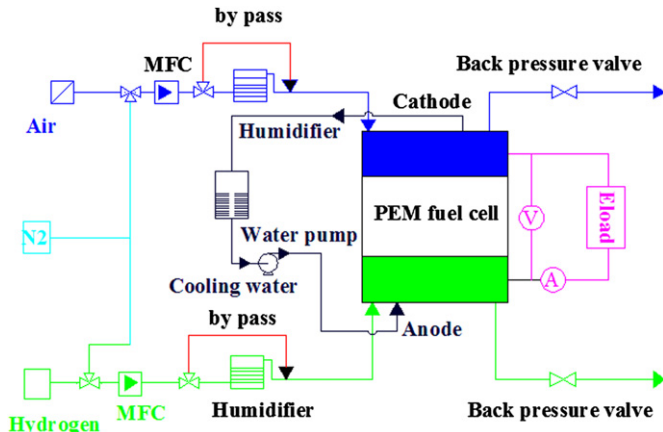


Fig. 1. Schematic diagram of the test system for PEM fuel cell stack.

2.2. Experiment scheme

In order to investigate the effect of the relative humidity (RH) on the liquid water recovery amount, three RH cases are designed. In addition, different numbers of the fans are applied to investigate the condensing capability of the condenser. As shown in Table 3, there are several different cases designed to investigate the water recovery amount from the stack. The fuel cell stack was pre-activated with increasing current on the stack with fully humidified H_2 /air for about 12 h before the polarization curves were recorded. After the activation process, polarization curve was recorded to evaluate the initial performance of the fuel cell stack. The detailed experimental conditions of the fuel cell stack are shown in Table 4.

3. Results and discussion

3.1. Voltage uniformity

Voltage uniformity was one of the most important representations of a well operated and assembled stack. The total power of the stack would be dropped if the voltage of one cell was extremely lower than the others. Fig. 3 showed the voltage uniformity in different RH conditions. As can be seen, when both air and hydrogen were completely humidified, the lowest voltage with a value of 0.650 V was observed at the eighty-fourth cell in the air inlet. The possible reason was that the temperature of the coolant water was lower than the inlet gas and the saturated water vapor was condensed into liquid water, which was not removed from the

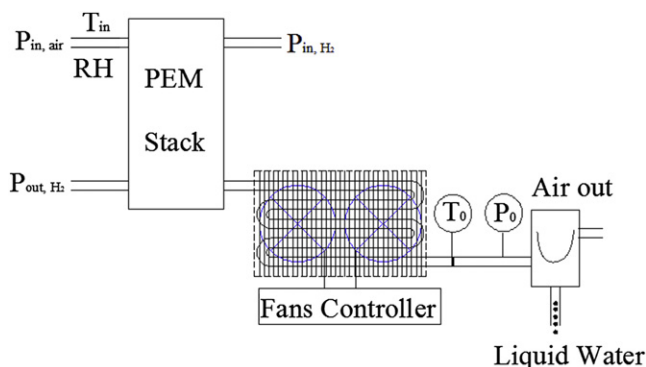


Fig. 2. Schematic diagram of the self-humidification process.

Table 2
Detail information of the condenser.

Condenser: FNF-7.1/30			
Length × width × height (mm)	Heat exchange area (m ²)	Fan	
		Number	Air flow rate (NLPM)
960 × 180 × 615	7.1	2	500

cell at a sufficient rate, resulting in the partial blockage of the pathways. When the humidity of air declined to 60%, the best voltage uniformity was achieved. While the hydrogen was not humidified, largest voltage oscillations were found among the cells. This might result from the transportation of water from the cathode to the anode to prevent dehydration of the membrane. Accordingly, the distribution of water inside the membrane was not uniform, leading to the varieties of the voltages. However, although the voltage distributions were different in three RH conditions, the average voltage and power were nearly the same as the values of 0.700 V and 5.92 kW, respectively, as shown in Table 5.

3.2. Water recovery

Fig. 4 displayed the time evolutions of liquid water collected from the outlet gas in different cases. As can be seen, the amount of water increased almost linearly with the time for all cases. When both hydrogen and air were completely humidified, the collected liquid water was about $0.435 \times 10^{-3} \text{ kg s}^{-1}$ in case 1, and it could increase to about $2.838 \times 10^{-3} \text{ kg s}^{-1}$ while one fan was operating to cool the gas, as shown in Table 6. Moreover, the generation of water was about $2.850 \times 10^{-3} \text{ kg s}^{-1}$ while two fans were used. Consequently, most of liquid water could be separated from the higher temperature gas in the condenser when the gas was cooled, and one fan should be enough for efficient separation of liquid water from the outlet gases. On the other hand, as can be seen in Table 5, the outlet temperature of the condenser in case 3 was about 7° higher than that in case 4, suggesting that water was mainly separated from the gas in the primary temperature decline, and the water separation rate decreased with the drop in the gas temperature in the condenser. At the end of the condensing process, there was almost no water could be separated from the gas.

Table 6 showed the amount of water generated from different aspects in different cases. With comparison of cases 5 and 4, higher relative humidity led to more water in the air. It was also obvious that the amount of recovered water was more than that for air humidification when the outlet gas was cooled, as described in Table 6. As a result, it was sufficient enough for air humidification of the stack. In addition, when RH was 60% in the air in case 5, the total amount of the water for air humidification and electrochemical reaction water was slightly less than that of the recovered water due to water transportation from the anode to the cathode through the membrane. On the contrast, the recovered water in case 6 was much less than that in case 4 when hydrogen was not humidified. Hence, water might transport from the cathode to the anode in case 6.

Table 3
Water recovery modes in different cases ($I = 100 \text{ A}$, $T_{in} = 343 \text{ K}$).

Cases	Fan number	RH _{air} (%)	RH _{H₂} (%)
Case 1	None	100	100
Case 2	None	100	0
Case 3	One	100	100
Case 4	Two	100	100
Case 5	Two	60	100
Case 6	Two	100	0

Table 4
Testing conditions of the experiments.

Reaction gas	Pure air and hydrogen
Flow rate of the gas (NLPM)	Hydrogen/air = 150/500
Gas inlet temperature (K)	Hydrogen/air = 343/343(70 °C)
Dew point (K)	343(70 °C)
Ambient temperature (K)	280(7 °C)
Current (A)	100

3.3. Separation temperature

3.3.1. Humidification water amount

Water in the outlet of the stack was mainly derived from three ways, i.e. the humidified water in the inlet, generated water from electrochemical reaction, and water transport in the PEM, water vapor content in the ambient air were all neglected in the following analysis. The mass flow rate of air and water in the inlet could be expressed as [23].

$$\dot{m}_a = \frac{n\lambda I}{0.21 \times 4 \times F} M_{\text{air}} \quad (1)$$

$$\dot{m}_{w,\text{add,air}} = \frac{M_{\text{H}_2\text{O}}}{M_{\text{air}}} \frac{p_{\text{in,H}_2\text{O}}}{p_{\text{in}} - p_{\text{in,H}_2\text{O}}} \dot{m}_a = \frac{n\lambda I}{0.21 \times 4 \times F} \cdot \frac{\text{RH} \cdot p_{\text{sat}}(T_{\text{in}})}{p_{\text{in}} - \text{RH} \cdot p_{\text{sat}}(T_{\text{in}})} \times M_{\text{H}_2\text{O}} = 1.19\lambda\phi \frac{nI}{F} M_{\text{H}_2\text{O}} \quad (2)$$

Where M_{air} and \dot{m}_a were the molecular weight and mass flow rate of the air, respectively, λ was the stoichiometry, n was the cell number, I was the working current, and F was the Faraday constant. p_{in} and $p_{\text{in,H}_2\text{O}}$ were the inlet total pressure and inlet water vapor partial pressure, respectively, $p_{\text{sat}}(T_{\text{in}})$ was the saturated water vapor pressure with respect to the inlet temperature T_{in} , RH was the relative humidity, $M_{\text{H}_2\text{O}}$ was the water molecular weight and $\phi = \text{RH} \cdot p_{\text{sat}}(T_{\text{in}})/(p_{\text{in}} - \text{RH} \cdot p_{\text{sat}}(T_{\text{in}}))$ was defined as the inlet humidity coefficient, representing the ratio of the inlet water vapor flow rate to the air flow rate. The mass flow rate of water generated from electrochemical reaction could be expressed as

$$\dot{m}_{w,\text{rea}} = \frac{nI}{2F} M_{\text{H}_2\text{O}} \quad (3)$$

Water transport in PEM generally includes electro-osmotic drag (EOD), back diffusion (BD), pressure driven hydraulic permeation (PDHE), and thermal-osmotic drag (TOD) [24]. Generally, it is not

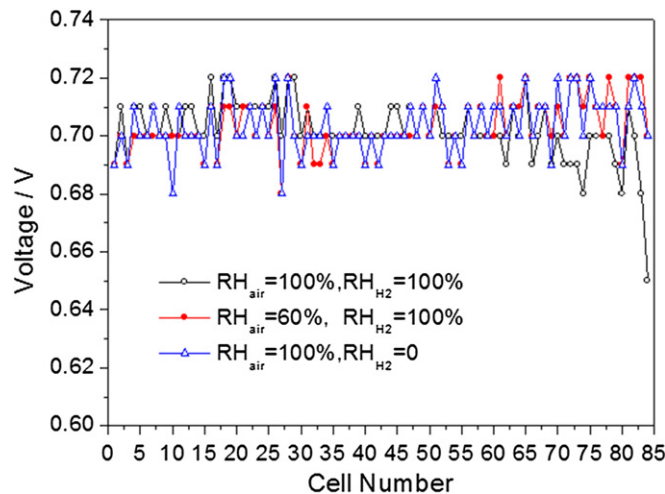


Fig. 3. Cell voltage uniformity in different RHs ($I = 100$ A, $T_{\text{in}} = 343$ K).

Table 5
Experimental data in different cases ($I = 100$ A, $T_{\text{in}} = 343$ K).

	$P_{\text{in,air}}$ (kPa)	T_0 (K)	P_c (10^3 W)	V_c (V)
Case 1	116.4	339	5.91	0.702
Case 2	115.2	336	5.92	0.699
Case 3	115.0	288	5.92	0.701
Case 4	115.2	281	5.91	0.700
Case 5	109.2	280	5.95	0.701
Case 6	114.6	282	5.93	0.699

easy to independently measure water transport coefficients. To simplify the process, the net drag coefficient (NDC) or net electro-osmotic drag coefficient is often used. The NDC is defined as the net number of water molecules dragged by each proton from the anode to the cathode. Assuming α is the net drag coefficient. Hence, the total mass flow rate of water (vapor and liquid) at the outlet of the stack was

$$\begin{aligned} \dot{m}_{w,\text{out}} &= \dot{m}_{w,\text{rea}} + \dot{m}_{w,\text{add,air}} + \dot{m}_{w,\text{EOD}} \\ &= [1.19\lambda\phi_{\text{air}} + 0.5 + \alpha] \frac{nI}{F} M_{\text{H}_2\text{O}} \end{aligned} \quad (4)$$

3.3.2. Water collection and air self-sufficient in water

The relationship of the saturated water vapor pressure p_{sat} (10^5 Pa) and the temperature T (K) could be expressed as [13]:

$$\begin{aligned} \lg p_{\text{sat}} &= -2.1794 + 2.953 \times 10^{-2}(T - 273) - 9.1837 \\ &\quad \times 10^{-5}(T - 273)^2 + 1.4454 \times 10^{-7}(T - 273)^3 \end{aligned} \quad (5)$$

Assuming that all the supersaturated water vapor can be condensed into liquid and flow into the water tank, then one could have

$$\frac{n_{0,\text{H}_2\text{O}}}{p_{\text{sat}}(T_0)} = \frac{\frac{n\lambda I}{0.21 \times 4 \times F} - \frac{nI}{4F}}{p_0 - p_{\text{sat}}(T_0)} \quad (6)$$

Where the numerator and denominator on the right were the molar flow rate and partial pressure of the non-water component, respectively, and the first term in the numerator was the molar flow rate of air in the inlet of the stack, the second term was the oxygen consuming molar rate during the reaction. p_0 was the outlet pressure of the condenser, $p_{\text{sat}}(T_0)$ and $n_{0,\text{H}_2\text{O}}$ were the saturated

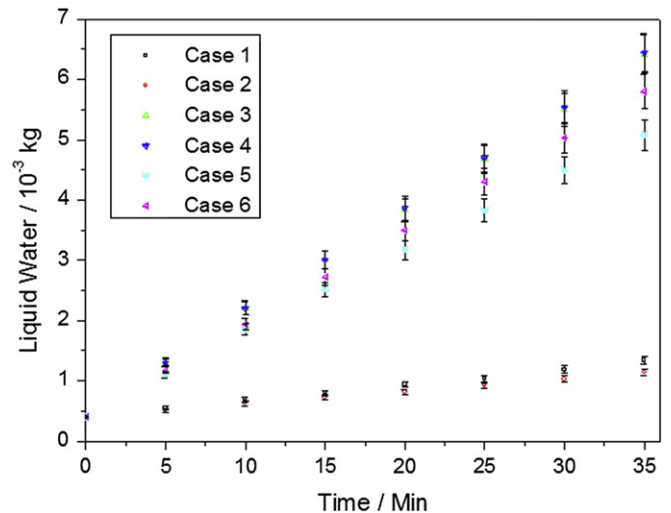


Fig. 4. Water recovery amount ($I = 100$ A, $T_{\text{in}} = 343$ K).

Table 6
Water recovery amounts in different cases ($I = 100$ A, $T_{in} = 343$ K).

	ϕ_{air}	$\dot{m}_{w,add,air}$ (10^{-3} kg s $^{-1}$) ^a	$\dot{m}_{w,rea}$ (10^{-3} kg s $^{-1}$) ^b	$\dot{m}_{w,rec}$ (10^{-3} kg s $^{-1}$) ^c
Case 1	0.358	2.397	0.785	0.435
Case 2	0.363	2.430	0.790	0.348
Case 3	0.364	2.438	0.788	2.838
Case 4	0.363	2.430	0.787	2.850
Case 5	0.198	1.327	0.793	2.233
Case 6	0.365	2.445	0.792	2.577

^a Calculated by Eq. (2).

^b Calculated by Eq. (3).

^c Linear fit in Fig. 4.

pressure and the molar flow rate of water vapor in the exhaust at the outlet of the condenser, respectively.

According to Eq. (6), one could obtain

$$n_{0,H_2O} = (1.19\lambda - 0.25) \frac{p_{sat}(T_0)}{p_0 - p_{sat}(T_0)} \frac{nI}{F} \quad (7)$$

Combining Eqs. (4) and (7), then the mass flow rate of the recovery liquid water at the outlet of the condenser could be expressed as

$$\begin{aligned} \dot{m}_{rec} &= \dot{m}_w - \dot{m}_{0,H_2O} \\ &= \left[1.19\lambda\phi + 0.5 + \alpha - (1.19\lambda - 0.25) \frac{p_{sat}(T_0)}{p_0 - p_{sat}(T_0)} \right] \frac{nI}{F} M_{H_2O} \end{aligned} \quad (8)$$

Accordingly, the criterion for self-humidification was

$$\begin{aligned} &\left[1.19\lambda\phi + 0.5 + \alpha - (1.19\lambda - 0.25) \frac{p_{sat}(T_0)}{p_0 - p_{sat}(T_0)} \right] \frac{nI}{F} M_{H_2O} \\ &\geq 1.19\lambda\phi \frac{nI}{F} M_{H_2O} \end{aligned} \quad (9)$$

Where the left term in the inequality was the mass flow rate of the recovery liquid water in the cathode, and the right term was the mass flow rate of the liquid water for air humidification.

Therefore, Eq. (9) could be simplified as

$$1 \leq \left[\frac{0.5 + \alpha}{1.19\lambda + 0.25 + \alpha} \right] \cdot \left[\frac{p_0}{p_{sat}(T_0)} \right] \quad (10)$$

Where the critical T_0 could be obtained by the joint solution of Eqs. (5) and (10).

3.3.3. Theoretical and experimental comparison

Fig. 5 showed the comparison between theoretical and experimental data for self-humidified temperature. Considering the NDC are ± 0.1 ($\pm 20\%$ of the amount of the reaction water), then the critical temperature deduced in Eq. (9) are 321 ± 4 K, respectively. Hence, the net drag coefficient (NDC) can be neglected in the theoretical analysis and the critical saturated pressure with respected to T_0 in Eq. (10) can be simply as:

$$p_{sat}(T_0) = \frac{0.5p_0}{1.19\lambda + 0.25} \quad (11)$$

As can be seen, the experimental data of the condenser outlet temperature was above the theoretical line (47.8 °C, calculated from Eq. (11)), indicating that the recovery water was not sufficient for the air humidification, such as cases 1 and 2. On the other hand, if the temperature was below the theoretical line, as for cases 3–6, it implied that the recovery water was sufficient for air humidification. In addition, the critical temperature was irrelevant with the

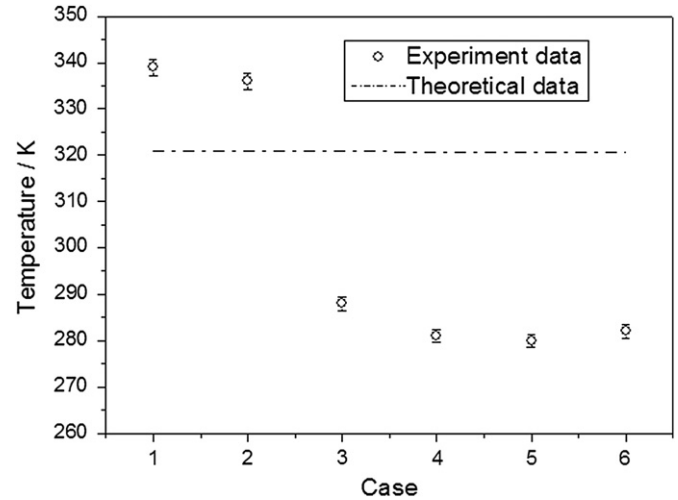


Fig. 5. Comparisons of the theoretical and experimental data ($I = 100$ A, $T_{in} = 343$ K).

stack power and voltage according to Eq. (10). Thus, the results described here could be used as the criteria for the air humidification in vehicle conditions.

3.3.4. Economics analysis

First of all, the condenser equipped with fans is widely used as the heat removal device in practical engineering due to its high heat removal capability and low price. The stack used in the experiment is 84 cells, and its power output ability can reach 10 kW or more, the cost of the stack is 10,000 CNY (10,000 ¥), while the condenser is less than 1000 CNY (1000 ¥). On the other hand, as mentioned above, the electricity used by each fan is 8 A, and the operation voltage is 24 V, so in our experiment, the additional capital cost is 1000 CNY, and the operation additional power is 384 W.

On the contrast, without of the condenser for the water recovery, according to Table 6, the additional water amount, usually low electrical conductivity deionized water or distilled water, for air humidification is about 2.4×10^{-3} kg s $^{-1}$ for a 6 kW stack, hence, the equipment cost for such a water produce capability will be 10 times [25] or more than that of a condenser, and the power cost, taking distilled water for instance whose latent heat is 2.4×10^6 kJ kg $^{-1}$, will reach 5.76 kW.

In all, our work provides an economic and convenient way to a realize the water balance in the fuel cell, water in the moisture can be separated to humidify the inlet gas sufficiently, and in this case, additional water is no longer needed in fuel cell operation, and the theoretical critical temperature for self-humidification can be easily obtain from the outlet pressure and reaction gas stoichiometry in fuel cell engineering.

4. Conclusions

To maintain an appropriate operation performance, the reaction gas is usually needed to be humidified. The mechanism of the air self-sufficient in water by condensing the outlet gas is presented in this paper, and some conclusions can be drawn:

Sufficient water can be recovered by condensing the high temperature exhaust of the stack, and the amount of recovered water can satisfy the humidification demand in the cathode easily by applying a high heat removal ability condenser.

The outlet temperature for self-humidification is irrelevant with the working current and cell number of the stack and it only depends on the inlet stoichiometry in atmospheric pressure.

Thus, just a single parameter is needed to be monitored. As a consequence, this method can be easily used for the air self-humidification in large power and long time operating fuel cell stacks.

Acknowledgements

This work is financially supported by the National Natural Science Foundation of China (Nos. 51036003, 51106046, and 50906026), Hunan Provincial Natural Science Foundation of China (No. 11JJ4032).

References

- [1] D.B. Kyung, S.K. Min, Characterization of nitrogen gas crossover through the membrane in proton-exchange membrane fuel cells, *International Journal of Hydrogen Energy* 36 (1) (2011) 732–739.
- [2] B. Mauricio, P.W. David, W. Haijiang, Application of water barrier layers in a proton exchange membrane fuel cell for improved water management at low humidity conditions, *International Journal of Hydrogen Energy* 36 (5) (2011) 3635–3648.
- [3] S.J. Peighambaroust, S. Rowshanzamira, M. Amjadi, Review of the proton exchange membranes for fuel cell applications, *International Journal of Hydrogen Energy* 35 (17) (2010) 9349–9384.
- [4] Y.J. Zhang, M.G. Ouyang, Q.C. Lu, et al., A model predicting performance of proton exchange membrane fuel cell stack thermal systems, *Applied Thermal Engineering* 24 (2004) 501–513.
- [5] P.H. Oosthuizen, L. Sun, K.B. McAuley, The effect of channel-to-channel gas crossover on the pressure and temperature distribution in PEM fuel cell flow plates, *Applied Thermal Engineering* 25 (2005) 1083–1096.
- [6] M.M. Hussain, I. Dincer, X. Li, A preliminary life cycle assessment of PEM fuel cell powered automobiles, *Applied Thermal Engineering* 27 (2007) 2294–2299.
- [7] B. Holley, A. Faghri, Permeability and effective pore radius measurements for heat pipe and fuel cell applications, *Applied Thermal Engineering* 26 (2006) 448–462.
- [8] L. Venturelli, P.E. Santangelo, P. Tartarini, Fuel cell systems and traditional technologies. Part II: experimental study on dynamic behavior of PEMFC in stationary power generation, *Applied Thermal Engineering* 29 (2009) 3469–3475.
- [9] S.G. Kandlikar, Z.J. Lu, Thermal management issues in a PEMFC stack – A brief review of current status, *Applied Thermal Engineering* 29 (2009) 1276–1280.
- [10] Y.T. Lee, Y.C. Kim, Y.H. Jiang, et al., Effects of external humidification on the performance of a polymer electrolyte fuel cell, *Journal of Mechanical Science and Technology* 21 (2007) 2188–2195.
- [11] S.H. Jung, S.L. Kim, M.S. Kim, et al., Experimental study of gas humidification with injectors for automotive PEM fuel cell systems, *Journal of Power Sources* 170 (2) (2007) 324–333.
- [12] P. Sridhar, R. Perumal, N. Rajalakshmi, et al., Humidification studies on polymer electrolyte membrane fuel cell, *Journal of Power Sources* 101 (1) (2001) 72–78.
- [13] T.E. Springer, T.A. Zawodzinski, S. Gottesfeld, Polymer electrolyte fuel cell model, *Journal of the Electrochemical Society* 138 (8) (1991) 2334–2342.
- [14] D.L. Wood, J.S. Yi, T.V. Nguyen, Effect of direct liquid water injection and interdigitated flow field on the performance of proton exchange membrane fuel cells, *Electrochimica Acta* 43 (24) (1998) 3795–3809.
- [15] D. Hyun, J. Kim, Study of external humidification method in proton exchange membrane fuel cell, *Journal of Power Sources* 126 (1–2) (2004) 98–103.
- [16] N. Rajalakshmi, P. Sridhar, K.S. Dhathathreyan, Identification and characterization of parameters for external humidification used in polymer electrolyte membrane fuel cells, *Journal of Power Sources* 109 (2) (2002) 452–457.
- [17] H.K. Lee, J.I. Kim, J.H. Park, et al., A study on self-humidifying PEMFC using Pt–ZrP–Nafion composite membrane, *Electrochimica Acta* 50 (23) (2004) 761–768.
- [18] T.H. Yang, Y.G. Yoon, C.S. Kim, et al., A novel preparation method for a self-humidifying polymer electrolyte membrane, *Journal of Power Sources* 106 (1–2) (2002) 328–332.
- [19] L. Wang, D.M. Xing, Y.H. Liu, et al., Pt/SiO₂ catalyst as an addition to Nafion/PTFE self-humidifying composite membrane, *Journal of Power Sources* 161 (1) (2006) 61–67.
- [20] M. Santis, D. Schmid, M. Ruge, et al., Modular stack-internal air humidification concept verification in a 1 kW Stack, *Fuel Cells* 4 (3) (2004) 214–218.
- [21] F.N. Büchi, S. Srinivasan, Operating proton exchange membrane fuel cells without external humidification of the reactant gases, *Journal of the Electrochemical Society* 144 (8) (1997) 2767–2772.
- [22] S.H. Ge, X.G. Li, I.M. Hsing, Internally humidified polymer electrolyte fuel cells using water absorbing sponge, *Electrochimica Acta* 50 (9) (2005) 1909–1916.
- [23] J. Larminie, A. Dicks, *Fuel Cell Systems Explained*, John Wiley & Sons Inc., New York, 2000.
- [24] W. Dai, H.J. Wang, X.Z. Yuan, et al., A review on water balance in the membrane electrode assembly of proton exchange membrane fuel cells, *International Journal of Hydrogen Energy* 34 (23) (2009) 9461–9478.
- [25] http://www.tka.de/en/applications/astm_iii_type_high_purity_water/ion_exchange_cartridges.

Nomenclature

- I : Working current (A)
 P_c : Stack power (W)
 V_c : Average voltage (V)
 RH : Relative humidity
 F : Faraday constant (96485C mol⁻¹)
 λ : Stoichiometry
 ϕ_{air} : Air inlet humidity coefficient
 α : Net drag coefficient
 T : Temperature (K)
 T_{in} : Inlet temperature (K)
 T_0 : Condenser outlet temperature (K)
 p_{in} : Stack inlet pressure (Pa)
 p_{sat} : Saturated water vapor pressure (Pa)
 p_0 : Condenser outlet pressure (Pa)
 p_{in,H_2O} : Inlet water vapor partial pressure (Pa)
 $p_{sat}(T_{in})$: Saturated water vapor pressure with respect to the inlet temperature (Pa)
 $p_{sat}(T_0)$: Saturated water vapor pressure with respect to the condenser outlet temperature (Pa)
 \dot{m}_a : Mass flow rate of air (kg s⁻¹)
 $\dot{m}_{w,add,air}$: Humidified water mass flow rate in the air (kg s⁻¹)
 $\dot{m}_{w,rea}$: Water mass flow rate generated from electrochemical reaction (kg s⁻¹)
 $\dot{m}_{w,rec}$: Mass flow rate of the recovery liquid water at the outlet of condenser (kg s⁻¹)
 M_{H_2O} : Molar weight of water (kg mol⁻¹)
 M_{air} : Molar weight of air (kg mol⁻¹)
 n_{0,H_2O} : Molar flow rate of the water at the condenser outlet (mol s⁻¹)
 \dot{n}_{0,H_2O} : Mass flow rate of water vapor at the outlet of the condenser (kg s⁻¹)